BUTTERWORTH HEINEMANN

Combined conduction, convection and radiation in a slot

C. Balaji and S. P. Venkateshan
Heat Transfer and Thermal Power Laboratory, Department of Mechanical Engineering, Indian Institute of Technology, Madras, India

This paper reports the results of a numerical study of the fundamental problem of combined mode heat transfer in a vertical slot. The paper is a sequel to the work of the authors on problems of interaction of natural convection with radiation and conduction in closed and open cavities. The present paper considers the intractions between all three modes of heat transfer and, hence, represents the most general case of interaction. The slot simulates a typical intermediate fin in a fin array or a typical section in an extruded heat sink commonly employed in practice. A detailed parametric study has led to useful correlations. The nature and extent of the coupling between the various modes of heat transfer are also elucidated.

Keywords: natural convection; conduction; radiation; coupling; slot; correlations

Introduction

Natural convection offers a quiet, reliable, and noiseless means of heat rejection from electrical equipment, electronic components, and packages. Natural convection heat sinks can be employed for heat fluxes up to about 1 kW/m^2. In most of these situations, convection is invariably coupled with conduction because of the finite thermal conductivity of the walls. To increase the heat transfer rates, the walls are usually coated with high emittance coating, thus introducing radiative coupling as well. A vertical slot representing an intermediate fin in a fin array or a typical section in a commercial heat sink is one such geometry commonly encountered in cooling applications. Lage et al. (1992) considered the effect of radiation in a slot but with one of the walls assumed to be isothermal (source) and the other walls assumed to be adiabatic, thus ignoring conduction effects. Chan and Tien (1985) made a numerical and an experimental investigation on a slot open at the side but ignoring the radiation and conduction effects. Balaji and Venkateshan (1994) have considered the effect of radiation coupling in a vertical slot, but the conjugate heat transfer in the wall was not considered. On the experimental side, free convection results for an array of vertical fins standing on a horizontal base have been reported by Starner and McManus (1963) and Harahap and McManus (1967), among others. However, there is no mention of radiation in either of the studies. The above two investigations were similar in conception and led to important conclusions regarding the flow pattern. The experimental results confirmed the presence of up and down flow pattern even when the spacing between the fins was only 0.01 m. The experiments were performed with fin heights of 0.01, 0.025, and 0.0375 m. The depth of the array was 10–20 times the fin height. For these geometric considerations, it was reported that up and down pattern was, indeed, observed. Actually, as the depth of the fin array system becomes larger, the up and down flow pattern dominates. In fact, Behnia and de Vahl Davis (1990) in their numerical study of the cooling of a microchip placed in a slot, have considered the flow to be up and down and also to be two-dimensional (2-D). Sobhan (1989) and Rammohan Rao (1992) used differential interferometry to study free convection from a three-dimensional (3-D) vertical fin array consisting of four fins standing on a horizontal base. The former presented results for three materials for both unsteady and steady convection for polished surfaces ($\varepsilon = 0.05$) for which radiation will be negligible. Fin material was found to affect convection heat transfer by about 10 percent in the range of parameters considered (aspect ratio = 1.4 and fin conductivity $30 \leq k_s \leq 205$ W/m K). Rammohan Rao studied the effect of radiation on heat transfer for the case of the fin material being aluminium and reported that for $\varepsilon = 0.85$, radiative heat transfer can contribute 45 percent of the total heat transfer, even when the source temperature is low, typically 373 K. However, the effect of conduction was not brought out because the study was performed for only one fin material.

A review of pertinent literature suggests that much work remains to be done both numerically and experimentally for the slot problem. Such work should take into account the interaction among all the three modes of heat transfer. Work needs to be done not only to gain further insight into the combined mode problem but also to develop correlations that will help in predicting overall heat transfer from such a system. Hence, the slot problem is far from being a closed issue. In the present study, the problem of combined mode heat transfer in such a slot has been taken up for a numerical investigation with a view to obtaining reasonably accurate values of heat transfer. The analysis is based on the assumption that the flow and temperature fields are 2-D. For a fin system that is very deep when compared to the height and when the spacing is typically between 0.025 and 0.07 m, more than twice the boundary-layer thickness, such an assumption seems reasonable.

Mathematical formulation

The geometry of the problem is given in Figure 1. The side walls are made of a material of finite thermal conductivity, and

Address reprint requests to Prof. S. P. Venkateshan at the Department of Mechanical Engineering, Indian Institute of Technology, Madras 600 036, India.

Received 26 April 1994; accepted 18 October 1994

Int. J. Heat and Fluid Flow 16: 139–144, 1995

655 Avenue of the Americas, New York, NY 10010

SSDI 0142-727X/95/$10.00
SSDI 0142-727X(94)00014-4

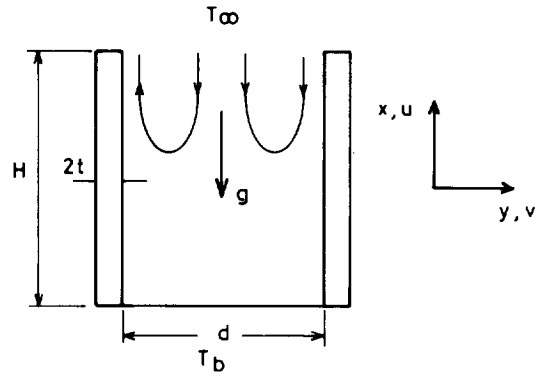

Figure 1 Problem geometry

they lose heat on both sides. The base (horizontal wall) is at a temperature T_B. The ambient is at T_∞ and $T_B > T_\infty$. Under the Boussinesq approximation, the governing equations for steady, 2-D, laminar, incompressible buoyancy induced flow with constant fluid properties under the vorticity stream function formulation in nondimensional form are given below. The temperature distribution on the left wall will be the same as that of the right wall in view of the symmetry.

$$U\,\partial\omega/\partial X + V\,\partial\omega/\partial Y = \mathrm{Pr}\,(\nabla^2\omega) - \mathrm{Ra_d}\,\partial\phi/\partial Y \tag{1}$$

$$\nabla^2\psi = -\mathrm{Pr}\,\omega \tag{2}$$

$$\nabla^2\phi = U\,\partial\phi/\partial X + V\,\partial\phi/\partial Y \tag{3}$$

The vorticity conditions on solid walls are well established (Gosman et al. 1969). For details regarding the flow conditions on the free boundaries, see Balaji and Venkateshan (1994). The details of the boundary conditions are given in Figure 2. In the ensuing section, a detailed discussion of the interaction (coupling) is presented.

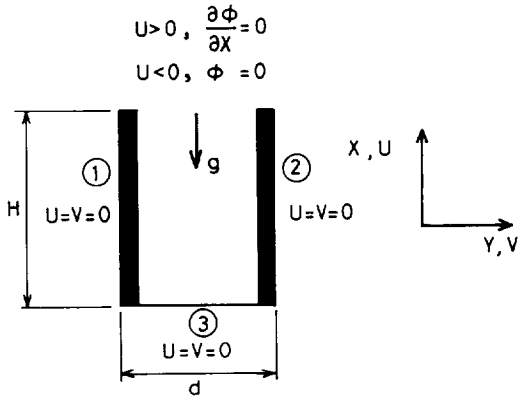

Figure 2 Details of boundary conditions

Modeling of coupling in side walls

A simple energy balance across a slice from the left wall results in the following equation in dimensionless form.

$$\partial^2\phi_s/\partial X^2 = -\gamma\,\partial\phi/\partial Y|_{Y=0} + \varepsilon\gamma N_{\mathrm{RC}}[(T/T_{\mathrm{B}})^4 - I] \tag{4}$$

where

$$\gamma = k_f d/k_s t \quad \text{and} \quad N_{\mathrm{RC}} = \sigma T_{\mathrm{B}}^4 d/k_f(T_{\mathrm{B}} - T_\infty).$$

Notation

A	aspect ratio, H/d
d	spacing or width, m
g	acceleration caused by gravity, m/s^2
H	height of the slot, m
I'	local irradiation, W/m^2
I	dimensionless irradiation, $I'/\sigma T_{\mathrm{B}}^4$
k_f	thermal conductivity of fluid, W/m K
k_s	thermal conductivity of wall material, W/m K
N_{RC}	radiation convection interaction parameter, $\sigma T_{\mathrm{B}}^4 d/k_f(T_B - T_\infty)$
Nu	convection Nusselt number based on d, $-(\partial\phi/\partial Y)_{Y=0}$ or $-(\partial\phi/\partial X)_{X=0}$
$\overline{\mathrm{Nu}}$	mean convection Nusselt number $\int_0^1 \mathrm{Nu}\,dY$ or $\int_0^A (\mathrm{Nu})/A\,dX$
$\overline{\mathrm{Nu}}$(tot)	Nusselt number (convection + radiation) based on d
$\mathrm{Nu_R}$	radiation Nusselt number, $\varepsilon N_{\mathrm{RC}}((T/T_B)^4 - I)$
$\overline{\mathrm{Nu_R}}$	mean radiation Nusselt number based on d, $\int_0^A \mathrm{Nu_R}/A\,dX$
Pr	Prandtl number, ν/α
$\mathrm{Ra_d}$	Rayleigh number based on d, $g\,\beta(T_B - T_\infty)\,d^3/\eta\alpha$
$\mathrm{Ra_H}$	Rayleigh number based on H, $\mathrm{Ra_d}\,A^3$
t	half thickness of the vertical wall, m
T	temperature, K
T_B	temperature of the base, K
T_∞	temperature of the ambient, K
T_{R}	temperature ratio, T_∞/T_{B}
T_{W}	wall temperature, K
u	vertical velocity, m/s
U	dimensionless vertical velocity, ud/α
v	horizontal or cross velocity, m/s
V	dimensionless horizontal velocity, vd/α
x	vertical coordinate, m
X	dimensionless vertical coordinate, x/d
y	horizontal coordinate, m
Y	dimensionless horizontal coordinate, y/d
Greek	
α	thermal diffusivity of the fluid, m^2/s
β	isobaric cubical expansion coefficient of fluid, 1/K
γ	thermal conductivity parameter, $(k_f\,d/k_s t)$
ε	total hemispherical emissivity of the walls
ν	kinematic viscosity of the fluid, m^2/s
σ	Stefan Boltzmann constant, 5.67×10^{-8} W/m^2 K^4
ϕ	dimensionless temperature, $(T - T_\infty)/(T_B - T_\infty)$
ϕ_s	dimensionless wall temperature, $(T_W - T_\infty)/(T_B - T_\infty)$
ψ'	stream function, m^2/s
ψ	dimensionless stream function, ψ'/α
ω'	vorticity, 1/s
ω	dimensionless vorticity, $\omega' d^2/\nu$

Equation 4 is a mathematical representation of the first law of thermodynamics applied to a wall element. The net heat conducted will be equal to the sum of the heat convected and radiated away. The parameter γ is termed the *thermal conductivity parameter*. It is the ratio of fluid conductance to solid conductance. The parameter N_{RC} is termed the *radiation convection parameter* and is the ratio of a representative black body radiative heat flux to a representative conduction heat transfer across the fluid layers. Several interesting limiting cases are possible as given below.

(1) In the absence of radiation ($\varepsilon = 0$) and γ tending to zero (this implies that the solid is of very high thermal conductivity) the right-hand side of Equation 4 vanishes. The wall is then at a uniform temperature.
(2) In the absence of radiation ($\varepsilon = 0$) and γ tending to infinity, Equation 4 reduces to $\partial\phi/\partial Y = 0$. This represents the case of an adiabatic wall.
(3) In the absence of radiation ($\varepsilon = 0$) and for finite values of γ, Equation 4 reduces to the classical conjugate convection problem.
(4) In the presence of radiation ($\varepsilon \neq 0$) for γ tending to infinity, the conjugate coupling becomes insignificant. The problem then becomes a radiation convection interaction problem. Such type of interactions are common for adiabatic walls and can be found in the analysis of such geometries as cavities, solar collectors, etc.
(5) In the presence of radiation ($\varepsilon \neq 0$) and very low values of γ, for instance $\gamma = 0$, when there is no fluid, such as in outer space, the problem represents the interaction of radiation and conduction. Such types of interactions are crucial in the design of space radiators.
(6) As a most general case when $\varepsilon \neq 0$ and γ is finite then the interaction between all the three modes of heat transfer is important. This general case has been taken up for consideration in the present study.

Method of solution

The governing Equations 1 and 3 subjected to the appropriate boundary conditions given in Figure 2 were solved using a finite volume method based on Gosman et al. (1969). Upwinding was used for the inertia terms to ensure that the coefficients that arise in the algorithm are always positive or at the worst, zero, and this ensures numerical stability and convergence. A 51 × 51 rectangular grid pattern with clustering in the vertical direction was used in the computation. Closely spaced grids are required near the bottom wall in view of the steep gradients in temperature. The grid pattern is shown in Figure 3. After every iteration of the convection solver, Equation 4 was solved by an explicit finite difference technique, and the new values are obtained for temperatures on the walls. These are used as boundary conditions for the next iteration of the convection solver. As regards the evaluation of the radiative terms that arise in Equation 4, the standard radiosity irradiation method was used. The grid pattern for convection was retained for radiation, and the required view factors were evaluated by the Hottel's crossed string method (Hottel and Saroffim 1967). An exactly similar procedure was used for radiation in an earlier investigation by the authors (Balaji and Venkateshan 1994). Calculations were stopped when the maximum difference in temperatures between successive iterations in any of the 2,601 nodes fell within 0.1 percent. The above specified accuracy was sufficient to obtain Nusselt numbers within an error of 1.5 percent. The local Nusselt numbers were obtained from the temperatures using the first derivatives, and the average Nusselt numbers were evaluated by numerical integration using trapezoidal rule. The local radiative Nusselt numbers Nu_R were evaluated from the relation $Nu_R = \varepsilon N_{RC}((T/T_B)^4 - 1)$, and the mean radiative Nusselt numbers $\overline{Nu_R}$ were evaluated using the trapezoidal rule.

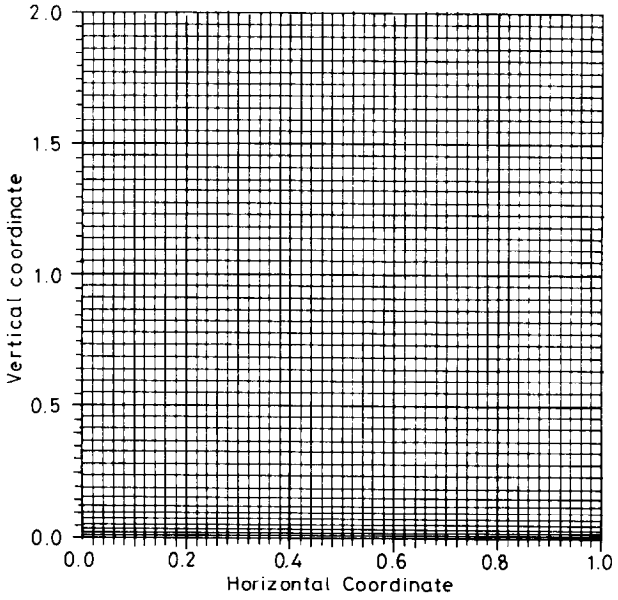

Figure 3 Grid pattern for $A = 2$

Results and discussion

Grid independence study

A series of calculations was done for the set of parameters given in Table 1 to determine the effect of grid size on the solution. From this exercise, it was found that the difference in Nusselt number obtained with a 51 × 51 grid and a 61 × 61 grid is only 1.8 percent; therefore, all the computations in the present study were done with a 51 × 51 grid.

Validation

For the case of the slot with adiabatic right and bottom walls and isothermal left wall, calculations were done for $\varepsilon = 0$, and the results correlated as $\overline{Nu_H} = 0.436\ Ra_H^{0.258}$. This compares well with the correlation $\overline{Nu_H} = 0.42\ Ra_H^{0.26}$, given by Lage et al. (1992). More detailed results for this geometry with nonzero emissivities are to be found in Balaji and Venkateshan (1994). When compared with the classical vertical flat plate case for which $\overline{Nu_H} = 0.59\ Ra_H^{0.25}$, the correlation for the open cavity ($0.436\ Ra_H^{0.258}$ or $0.42\ Ra_H^{0.26}$) predicts a Nusselt number 18–20 percent smaller. This is because, for vertical slot, the fluid cannot enter the slot from the bottom and the sides. The flowfield is shown in Figure 1. It was also observed that as A increases (all other conditions remaining fixed), the heat

Table 1 Results of the grid independence study ($\gamma = 0.01$, $Ra_d = 9.6 \times 10^5$, $Pr = 0.71$, $A = 2$, $\varepsilon = 0$)

Grid	Nu_d
41 × 41	10.91
51 × 51	11.80
61 × 61	12.02

transfer rates drop consistent with the above and with the fact that wall boundary layers tend to restrict the incoming flow.

Flow and heat transfer characteristics

Figure 4 shows the variation of vertical velocity at the top of the slot for the set of parameters shown in the figure. It can be seen that the flow enters from the top in the middle of the slot and rises symmetrically near the vertical walls. The velocity profile satisfies the mass balance across the opening; i.e., fluid flow into the slot is equal to the fluid flow out of the slot. The temperature distribution across the top for the same case is shown in Figure 5. The figure confirms the prevalence of boundary-layer type of flow, and roughly half of the opening area is at the ambient temperature. Hence, there is absolutely

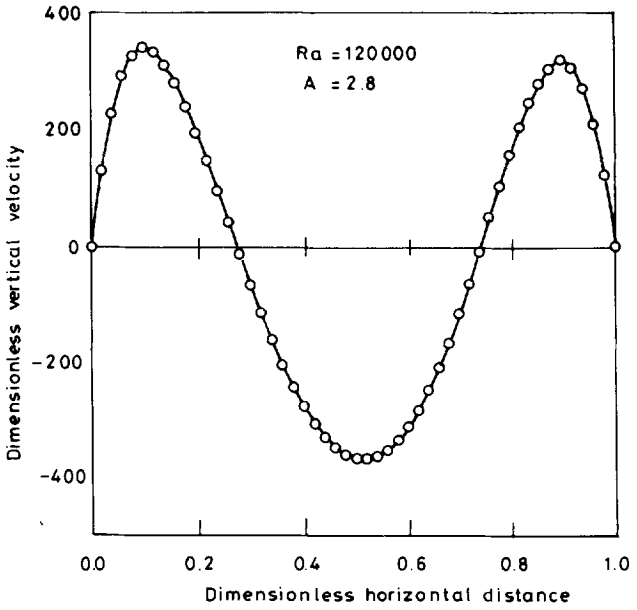

Figure 4 Variation of vertical velocity at the top for $\gamma = 0.005$ and $\varepsilon = 0$

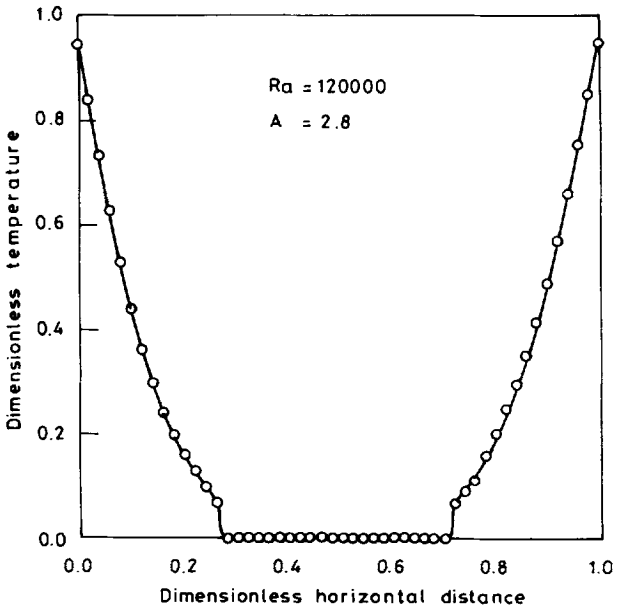

Figure 5 Variation of dimensionless temperature at the top for $\gamma = 0.005$ and $\varepsilon = 0$

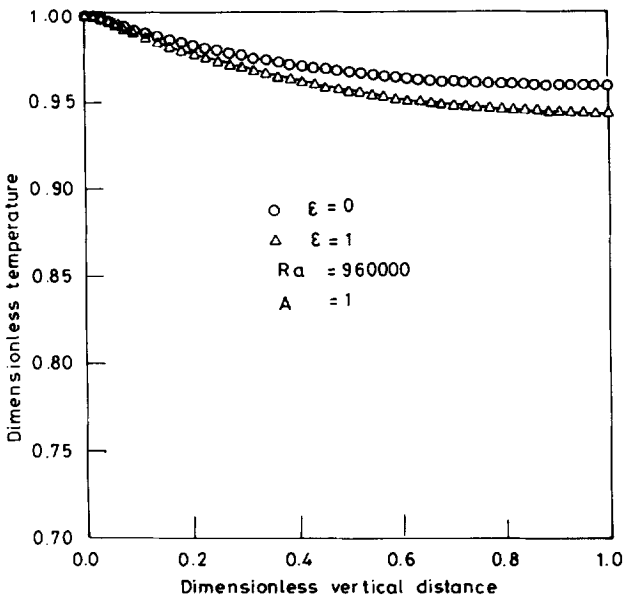

Figure 6 Temperature profile along the vertical wall for two different wall emissivities for $\gamma = 0.005$

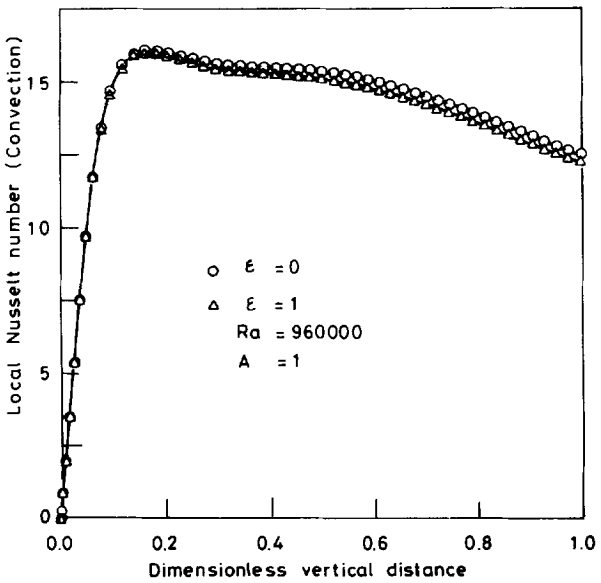

Figure 7 Local Nusselt number distribution along the vertical wall for two different wall emissivities for $\gamma = 0.005$

no interaction between the boundary layers on the left and right walls. However, the temperature distribution along the side walls depends on the conduction as well as radiative coupling. Therefore, we can still say that there is an interaction as regards the two side walls. The effect of radiation can be explicitly seen in Figures 6 and 7. The temperature distribution and the Nusselt number distribution along the side walls are shown respectively in these two figures. Radiation has a relatively weak influence on both the temperature as well as convective heat transfer. From a physical standpoint, this is justifiable. The thermal conductivity of the wall material being high, the problem under consideration becomes more a conduction convection interaction problem. In addition, the vertical side walls tend to reduce the radiative heat transfer from the base. In other words, for highly emitting walls, the base, in the absence of the vertical walls, will lose more heat

radiatively than when the side walls are present. Even so, the convective heat transfer increases because of the presence of side walls. Thus, from the standpoint of overall heat transfer, the slot arrangement will certainly lose more heat than the base surface alone. Therefore, it is also apparent that radiation can be decoupled and computed separately once the conjugate problem of combined conduction and convection has been solved. The error incurred by doing this, on the overall heat transfer, will only be a few percentage points and insignificant in engineering terms. It is worth while looking into the effect of the conductive–convective coupling on the temperature and Nusselt number distributions. This coupling is a strong function of the thermal conductivity of the side walls. For a material with $k_s = 30$ W/m K, $2t = 0.0015$ m and in air, the tip temperature can be 18–20°C less than the base temperature (Figure 8). For the same case, the Nusselt number is smaller

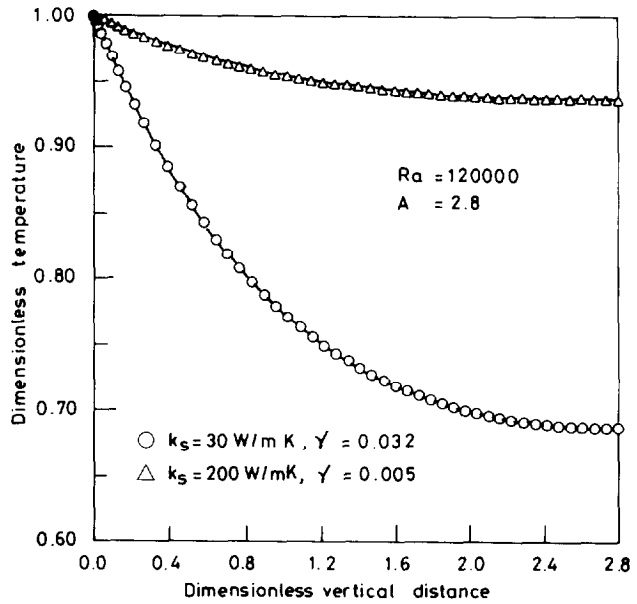

Figure 8 Temperature profile along the vertical wall for two different wall materials ($2t = 0.0015$ m)

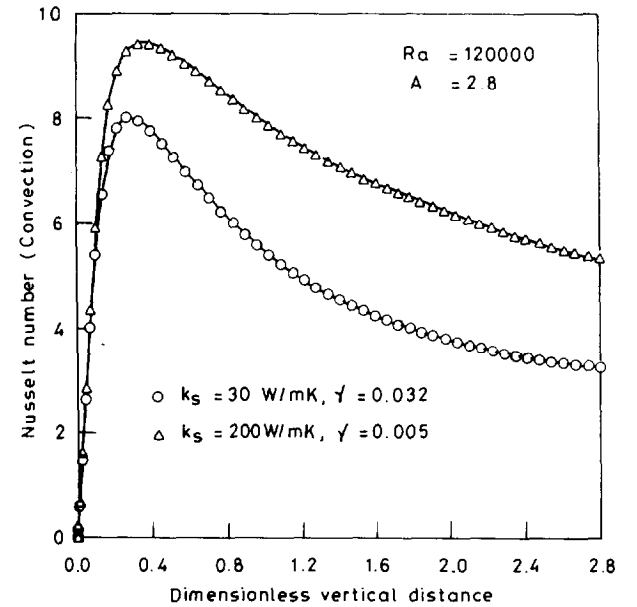

Figure 9 Local Nusselt number distribution along the vertical wall for two different wall materials ($2t = 0.0015$ m)

Table 2 Range of parameters in the present study (numerical; Pr = 0.71)

$0.005 \leq \gamma \leq 0.07$
$1 \times 10^5 \leq Ra_d \leq 1 \times 10^6$
$1 \leq A \leq 3$
$0 \leq \varepsilon \leq 1$
$0.75 \leq T_R \leq 0.90$

by as much as 30 percent than that for isothermal vertical walls (Figure 9). The Nusselt number distribution shows a nonmonotonic variation as opposed to the vertical isothermal plate case. The nonisothermal vertical walls and the presence of the base change the flowfield significantly and, thus, the typical variation. Rammohan Rao (1992) and Sobhan (1989) have observed such variation in their experimental studies. Hence, it is essential that the conduction–convection coupling is considered in this problem. On the other hand, radiation coupling is not significant. However, once the conduction–convection coupling is built into the numerical scheme, the scheme can be extended to include radiation without a great deal of additional computational effort.

Correlations

Based on a parametric study, correlations were developed for both convective and radiative heat transfer rates. The range of parameters for which calculations have been done are given in Table 2. In all, about 22 cases were considered in arriving at the correlation.

Convection. *(1) Side wall heat transfer:*

$$\overline{Nu}_C = 0.36\ Ra_d^{0.273}[1/(1+\gamma)]^{13.02}A^{-0.215} \tag{5}$$

(2) Base heat transfer:

$$\overline{Nu}_C(\text{base}) = 0.626\ Ra_d^{0.215}[1/(1+\gamma)]^{0.019}A^{0.168} \tag{6}$$

The correlations were chosen in the above form so that they bring out the salient features of the heat transfer problem. The Rayleigh number exponent of 0.273 in Equation 5 is consistent with the normally encountered exponents for laminar buoyancy induced flows over vertical surfaces, and these usually range between 0.25 and 0.30. The effect of aspect ratio is predictable, because an increase in aspect ratio results in larger boundary layer thicknesses, and hence in view of this, there will be lesser entrainment from the top. The thermal conductivity parameter γ has a very strong effect on the sidewall heat transfer, and the form was intentionally chosen so that as γ tends to zero, this term reduces to unity. Because the base is isothermal, the conjugate coupling should have very negligible effect on the base heat transfer, and hence Equation 6 shows a very weak dependence on γ. The aspect ratio has an exponent of 0.168. For the same spacing, the side walls of a higher aspect ratio cavity will show more deviation from the isothermal condition as opposed to a lower aspect ratio cavity. Also, the heat transfer to the fluid layers is mainly from the side walls. Therefore, if we consider temperature profiles across the cavity at a horizontal plane near the base for both the cases, the higher aspect ratio cavity will show a lower temperature at all the stations compared to the lower aspect ratio cavity. However, the base is at the same temperature for both the cases. In view of this, the driving temperature difference for convection from the base is more for the higher aspect ratio case, thus it will lose more heat. This explains the positive exponent of the aspect ratio in Equation 6. However, it must be mentioned that the effect of aspect ratio on the base heat transfer is no more than 20 percent for the range of parameters considered. The Rayleigh

number exponent of 0.215 in Equation 6 is comparable to the usual value (0.25) for horizontal surfaces. Both the correlations had correlation coefficients over 99 percent and the error bands were ± 4 percent.

Radiation. *(1) Side wall heat transfer:*

$$\overline{Nu}_R = 1.66\varepsilon^{0.36}[1/(1+\gamma)]^{4.25}(1 - T_R^4)^{0.33}N_{RC}^{0.36}A^{-1.416} \quad (8)$$

(2) Base heat transfer:

$$\overline{Nu}_R = 0.188\varepsilon^{0.66}[1/(1+\gamma)]^{-6.15}(1 - T_R^4)^{1.15}N_{RC}^{1.26}A^{-0.286} \quad (9)$$

The correlations above had a correlation coefficient over 99 percent and the error band was ± 3 percent. If we look at Equation 9 the N_{RC} term has an exponent of 1.26, which represents only a slight departure from unity. This departure is caused by the presence of nonisothermal side walls. The form $(1 - T_R^4)$ was chosen because radiative flux is always proportional to $(T_B^4 - T_\infty^4)$. The exponent of 1.15 is also close to 1. The parameter γ was chosen in the present form for reasons already mentioned. The exponent of emissivity is 0.66 because of the multiple reflections within the slot, irradiations from the sides, and the restricted exposure of the base to the ambient. As might be expected, at higher aspect ratios, radiative Nusselt numbers decrease for the aforementioned reasons. The parameter γ has a negative exponent of -6.15. This is because for larger γ, the side walls depart considerably from isothermal condition, and hence irradiations on the base decrease. Therefore, there is an increase in $\overline{Nu}_R$(base). Similarly, Equation 8, which gives $\overline{Nu}_R$ from the side wall, shows an exponent of 0.36 for ε. This severe reduction in the exponent is mainly attributable to the nonisothermal nature of the wall, irradiations from the base and the other side (right side for left and vice versa), and the restricted view factor to the ambient. The above reasons also hold true for the exponents of γ, N_{RC} and T_R. Because both N_{RC} and T_R are based on T_B as the source temperature, it is clear that because of the conjugate coupling, there is a temperature drop along the side wall, and hence T_B is no longer the reference temperature. However, because T_B and T_∞ represent the upper and lower limits of temperature in the problem under consideration, the terms N_{RC} and T_R can still be used for correlating the results, but their exponents will be far from 1. For similar reasons, the aspect ratio term has a negative exponent. In fact, the correlation for the side wall shows, predictably, more severe dependence on A.

General discussion

In this paper, the interaction of all the three modes of heat transfer in a slot was considered. The computations were performed for laminar flow. It is fairly apparent that as far as laminar natural convection is concerned, scope for future work in this area is virtually exhausted. However, when the fluid flow is turbulent, the results may be interesting, and this opens new vistas for further research in this area. In a series of papers on this area of research, the authors have demonstrated the use of finite volume method for the interaction problems. The suitability of the vorticity stream function approach for this class of problems was also established. In all the investigations, the algorithm from Gosman et al. (1969) was employed and was found to give stable and accurate results for all the problems considered, with less computational effort as compared to the primitive variable approach that would generally involve a larger number of grids in the computational domain (see, for example, Lage et al. 1992 and discussion on Lage et al. by Balaji and Venkateshan 1993). However, it must be mentioned that the vorticity–stream function method becomes highly cumbersome and unsuitable for handling 3-D flows. This is so because vorticities in three directions must be defined, and the advantage in eliminating the pressure terms is more than offset by the increase in computational effort. The primitive variable approach is likely to be more advantageous for these problems.

Conclusions

A numerical investigation of combined conduction, convection, and radiation in a slot was performed using a finite volume method. The study has demonstrated the significance of the conjugate coupling in determining both the convective and radiative heat transfer rates. Although radiation itself can contribute up to 30 percent of the total heat transfer, radiation coupling was found not be severe. In view of this, radiation can be decoupled without any significant loss of accuracy. Correlations were developed for the convective and radiative heat transfer rates from the slot. The various terms in the correlation were chosen after careful consideration;. A detailed discussion of these correlations has provided much insight into the physics of the problem.

References

Balaji, C. and Venkateshan, S. P. 1993. Discussion on natural convection with radiation in a cavity with open top end. *J. Heat Transfer*, **115**, 1085–1086

Balaji, C. and Venkateshan, S. P. 1994. Interaction of surface radiation with free convection in an open cavity. *Int. J. Heat Fluid Flow*, **15**, 317–324

Behnia, M. and de Vahl Davis, G. 1990. Natural convection cooling of an electronic component in a slot. *Proc. 9th Int. Heat Transfer Conf.*, Hemisphere Publishing Corp., New York, **2**, 343–348

Chan, Y. L. and Tien, C. L. 1985. A numerical study of two-dimensional laminar natural convection in shallow open cavities. *Int. J. Heat and Mass Transfer*, **28**, 601–612

Gosman, A. D., Pun, W. M., Runchal, A. K., Spalding, D. B. and Wolfshtein, M. 1969. *Heat and Mass Transfer in Recirculating Flows*, Academic Press, London

Harahap, F. and McManus, H. N. 1967. Natural convection heat transfer from horizontal rectangular fin arrays. *J. Heat Transfer*, **89**, 32–38

Hottel, H. C. and Saroffim, A. F. 1967. *Radiative Heat Transfer*, McGraw-Hill, New York, 31–39

Lage, J. L., Lim, J. S. and Bejan, A. 1992. Natural convection with radiation in a cavity with open top end. *J. Heat Transfer*, **114**, 479–486

Rammohan Rao, V. 1992. Interferometric study of interaction between radiation and free convection in fins and fin arrays. Ph.D thesis, Department of Mechanical Engineering, Indian Institute of Technology, Madras, India

Sobhan, C. B. 1989. Free convection studies on horizontal fins and fin arrays via differential interferometry. Ph.D. thesis, Department of Mechanical Engineering, Indian Institute of Technology, Madras, India

Starner, K. E. and McManus, H. N. 1963. An experimental investigation of free convection from rectangular fin arrays. *J. Heat Transfer*, **85**, 273–278